
DiffusionShield: A Watermark for Copyright Protection against Generative Diffusion Models

Yingqian Cui*

Michigan State University
cuiyingq@msu.edu

Jie Ren*

Michigan State University
renjie3@msu.edu

Han Xu

Michigan State University
xuhan1@msu.edu

Pengfei He

Michigan State University
hepengf1@msu.edu

Hui Liu

Michigan State University
liuhui7@msu.edu

Lichao Sun

Lehigh University
lis221@lehigh.edu

Jiliang Tang

Michigan State University
tangjili@msu.edu

Abstract

Recently, Generative Diffusion Models (GDMs) have showcased their remarkable capabilities in learning and generating images. A large community of GDMs has naturally emerged, further promoting the diversified applications of GDMs in various fields. However, this unrestricted proliferation has raised serious concerns about copyright protection. For example, artists including painters and photographers are becoming increasingly concerned that GDMs could effortlessly replicate their unique creative works without authorization. In response to these challenges, we introduce a novel watermarking scheme, DiffusionShield, tailored for GDMs. DiffusionShield protects images from copyright infringement by GDMs through encoding the ownership information into an imperceptible watermark and injecting it into the images. Its watermark can be easily learned by GDMs and will be reproduced in their generated images. By detecting the watermark from generated images, copyright infringement can be exposed with evidence. Benefiting from the uniformity of the watermarks and the joint optimization method, DiffusionShield ensures low distortion of the original image, high watermark detection performance, and the ability to embed lengthy messages. We conduct rigorous and comprehensive experiments to show the effectiveness of DiffusionShield in defending against infringement by GDMs and its superiority over traditional watermarking methods.

1 Introduction

Generative diffusion models (GDMs), such as Denoising Diffusion Probabilistic Models (DDPM) Ho et al. [2020] have shown their great potential in generating high-quality images. This has also led to the growth of more advanced techniques, such as DALL·E2 [Ramesh et al., 2022], Stable Diffusion [Rombach et al., 2022], and ControlNet [Zhang and Agrawala, 2023]. In general, a GDM learns the distribution of a set of collected images, and makes samplings to generate images that follow the learned distribution. As these techniques become increasingly popular, concerns have arisen regarding the copyright protection of creative works shared on the Internet. For instance, a fashion company may invest significant resources in designing a new fashion. After the company posts the pictures of this fashion to the public for browsing, an unauthorized entity can train their

*Equal contribution

GDMs to mimic its style and appearance, generating similar images and resulting in products. This infringement highlights the pressing need for copyright protection mechanisms.

To provide protection for creative works, watermark techniques such as Cox et al. [2002], Podilchuk and Delp [2001], Zhu et al. [2018], Navas et al. [2008], Yu et al. [2021] are often deployed, which aim to inject (invisible) watermarks into images and then detect them to track the malicious copy and accuse the infringement. However, directly applying these existing methods to GDMs still faces tremendous challenges. Indeed, since existing watermark methods have not specifically been designed for GDMs, their watermarks in the original images could be eliminated by the denoising process of GDMs so they could disappear in GDM-generated images. Then, the infringement cannot be effectively verified and accused. As empirical evidence in Figure 1, we train two popular GDMs on a CIFAR10 dataset whose samples are watermarked by two representative watermark methods [Navas et al., 2008, Zhu et al., 2018], and we try to detect the watermarks in the GDM-generated images. The result demonstrates that the watermarks from these methods are either hardly learned and reproduced by GDM (e.g., FRQ Navas et al. [2008]), or require a very large budget (the extent of image distortion) to partially maintain the watermarks (e.g., HiDDeN [Zhu et al., 2018]). Therefore, dedicated efforts are still greatly desired to developing the watermark technique tailored for GDMs.

In this work, we argue that one critical factor that causes the inefficacy of these existing watermark techniques is the inconsistency of watermark patterns. It means that, in these methods [Navas et al., 2008, Zhu et al., 2018], the watermark in each image for each user is distinct. Thus, GDMs can hardly learn the distribution of watermarks and reproduce them in the generated samples. To address this challenge, we propose **DiffusionShield** to successfully enhance the “*pattern uniformity*” (Section 3.2) of the watermarks to make them consistent and easily reproduced by GDMs. Different from existing methods, DiffusionShield manages to increase this “*pattern uniformity*” by designing **blockwise watermarks** that are divided into basis patches. Each user can have a specified sequence of these basis patches to watermark his / her images, identifying the unique copyright. As a result, the watermarks will repeatedly appear in the training set of GDMs, to make them be reproducible and detectable. Furthermore, DiffusionShield introduces a joint optimization method for basis patches and the watermark detector to enhance each other, which achieves protection with a smaller budget and higher accuracy. In addition, once the watermarks are obtained, DiffusionShield does not require re-training when there is an influx of new users and images. As a result, DiffusionShield enables great flexibility to accommodate multiple users. To the best of our knowledge, this work is the first one that accomplishes the goal to protect the copyright of data against GDMs via watermark techniques.

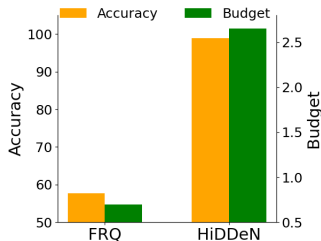


Figure 1: Watermark detection accuracy (%) on GDM-generated images and the corresponding budget (l_2 norm) of watermarks.

2 Related Work

2.1 Generative Diffusion Models (GDM)s

In recent years, Generative Diffusion Models (GDMs) have made significant strides. A breakthrough in GDMs is achieved by DDPM Dhariwal and Nichol [2021], which demonstrates great superiority in generating high-quality images. The work of Ho and Salimans [2022] further advances the field by proposing a novel approach that eliminates the need for classifiers in the training process of GDMs. The work Song et al. [2020] presents Denoising Diffusion Implicit Models (DDIMs), a variant of GDMs with improved efficiency in sampling. Besides, techniques such as Rombach et al. [2022] achieve high-resolution image synthesis and text-to-image synthesis by applying the diffusion processes in the latent space of images. These advancements underscore the growing popularity and efficacy of GDM-based techniques.

To train Generative Diffusion Models (GDMs), many existing methods rely on collecting a significant amount of training data from public resources [Deng et al., 2009, Yu et al., 2015, Guo et al., 2016]. However, there is a concern that if a GDM is trained on copyrighted material and produces outputs that are substantially similar to the original copyrighted works, it could potentially infringe on the copyright owner’s rights. This issue has already garnered public attention Vincent [2023]. This paper focuses on mitigating this risk by employing a watermarking technique to detect copyright infringements associated with GDMs.

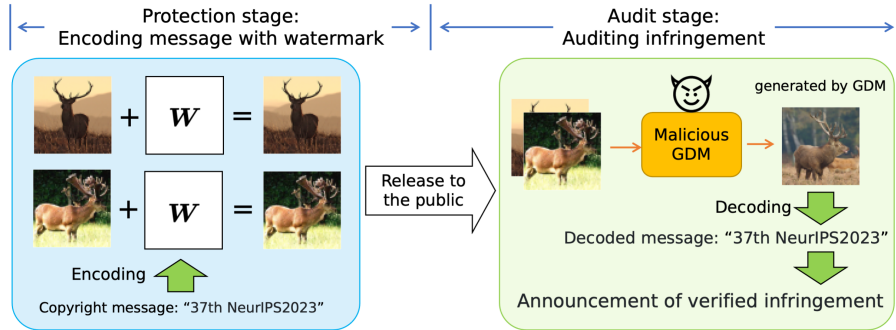


Figure 2: An overview of watermarking against GDM that consists of two stages.

2.2 Image Watermarking

Image watermarking involves embedding invisible information into the carrier images and is commonly used to identify ownership of the copyright. Traditional watermarking techniques include spatial domain methods and frequency domain methods Cox et al. [2002], Navas et al. [2008], Shih and Wu [2003], Kumar [2020]. These techniques embed watermark information by modifying the pixel values Cox et al. [2002], frequency coefficients Navas et al. [2008], or a combination of both Shih and Wu [2003], Kumar [2020]. In recent years, various digital watermarking approaches based on Deep Neural Networks (DNNs) Zhu et al. [2018], Zhang et al. [2019], Tancik et al. [2020], Weng et al. [2019] have been proposed. For example, an autoencoder-based network architecture is introduced to conduct the embedding and extracting of watermarks Zhu et al. [2018], while the structure of GAN is utilized Zhang et al. [2019] to realize high-capacity imperceptible watermark embedding. Those techniques are then further generalized to physical photographs Tancik et al. [2020] or videos Weng et al. [2019].

Notably, there are existing studies focusing on watermarking generative neural networks, such as GANs [Goodfellow et al., 2020] and image processing networks [Sehwag et al., 2022]. Different from our work, their goal is to safeguard the *intellectual property (IP) of generative neural networks* or to make synthetic images distinguishable from natural images to *prevent the spread of visual misinformation*. To accomplish their goals, the works Wu et al. [2020], Yu et al. [2021], Zhao et al. [2023a], Zhang et al. [2020] embed imperceptible watermarks into every output of a generative model, enabling the defender to determine whether an image was generated by a specific model or not. Various approaches have been employed to inject watermarks, including reformulating the training objectives of the generative models Wu et al. [2020], modifying the model’s training data Yu et al. [2021], Zhao et al. [2023a], or directly applying a watermark embedding process to the output images before they are presented to end-users Zhang et al. [2020].

Additionally, a backdoor trigger is extended to protect data by Li et al. [2022]. However, it has been designed solely for classification models instead of GDMs, and cannot be applied to our task since it does not encode any text information about the copyright and requires the access to the suspicious model. In this paper, we delve into the development of watermarks specifically designed for GDMs with the principal aim of safeguarding the copyright of data against potential infringement by these GDMs. This could be a more difficult problem as the data owners cannot control the training and the inference process of GDMs.

3 Method

In this section, we first formally define our studied problem and the key notations. Next, we point out that the “pattern uniformity” is a key factor for the watermark to be reproduced in GDM-generated samples. Based on this finding, we introduce the details for the two essential components of our watermarking method DiffusionShield, i.e., the blockwise watermark with pattern uniformity and the joint optimization, respectively.

3.1 Problem Statement

In this work, we consider there are two roles: (1) **a data owner** who holds the copyright of the data, releases them solely for public browsing, and aspires to protect them from being replicated by GDMs, and (2) **a data offender** who employs a GDM on the released data to appropriate the creative works and infringe the copyright. In reality, we often collect data from multiple resources to train GDMs.

Thus, we consider a scenario where there are multiple owners to protect their copyright against GDMs by encoding the copyright information into watermarks. We start by defining the one-owner case, and then extend the discussion to the multiple-owner case:

• **Protection for one-owner case.** An image owner aims to release n images, $\{\mathbf{X}_{1:n}\}$, strictly for browsing. Each image \mathbf{X}_i has a shape of (U, V) where U and V are the height and width, respectively. As shown in Figure 2, the protection process generally comprises two stages: 1) *a protection stage* when the owner encodes the copyright information into the invisible watermark and adds it to the protected data; and 2) *an audit stage* when the owner examines whether a GDM-generated sample infringes upon their data. In the following, we introduce crucial definitions and notations.

- 1) *The protection stage* happens before the owner releases $\{\mathbf{X}_{1:n}\}$ to the public. To protect the copyright, the owner encodes the copyright message M into an invisible watermark \mathbf{W}_i , and adds the watermark into \mathbf{X}_i to get a protected data $\tilde{\mathbf{X}}_i = \mathbf{X}_i + \mathbf{W}_i$. M can contain information like texts which can signify the owners’ unique copyright. $\tilde{\mathbf{X}}_i$ and \mathbf{X} appear similar in human eyes because the budget of the watermark is restrained by $\|\mathbf{W}_i\|_p \leq \epsilon$. Hence, the watermark does not detrimentally affect normal browsing. Instead of releasing $\{\mathbf{X}_{1:n}\}$, the owner releases the protected $\{\tilde{\mathbf{X}}_{1:n}\}$ for public browsing.
- 2) *The audit stage* refers to the scenario that the owner finds suspicious images which potentially offend the copyright of their images, and they scrutinize whether these images are generated by GDMs from their released data. We assume that the data offender collects a dataset $\{\mathbf{X}_{1:N}^G\}$ that contains the protected images $\{\tilde{\mathbf{X}}_{1:n}\}$, i.e. $\{\tilde{\mathbf{X}}_{1:n}\} \subset \{\mathbf{X}_{1:N}^G\}$ where N is the total number of both protected and unprotected images, and trains a GDM, \mathcal{G} , from scratch to generate images, \mathbf{X}_G , which mimics the protected images. If \mathbf{X}_G contains the copyright information of the data owner, once \mathbf{X}_G is inputted to a decoder \mathcal{D} , the copyright message should be decoded by \mathcal{D} . Notably, the data owner is not required to have access to \mathcal{G} during this stage.

• **Protection for multiple-owner case.** When there are K data owners to protect their distinct sets of images, we denote their sets of images as $\{\mathbf{X}_{1:n}^k\}$ where $k = 1, \dots, K$. Following the methodology of one-owner case, each owner can re-use the same encoding process and decoder to encode and decode distinct messages in different watermarks, \mathbf{W}_i^k , which signifies their specific copyright messages M^k . The protected version of images is denoted by $\tilde{\mathbf{X}}_i^k = \mathbf{X}_i^k + \mathbf{W}_i^k$. Then the protected images, $\{\tilde{\mathbf{X}}_{1:n}^k\}$, can be released by their respective owners for public browsing, ensuring their copyright is maintained. More details about the two protection cases can be found in Appendix A.

3.2 Pattern Uniformity

In this subsection, we uncover one important factor which we called “*pattern uniformity*” that could be an important reason for the failure of existing watermark techniques in GDMs. Before our work, there are previous studies Sehwaq et al. [2022], Um and Ye [2023], Daras et al. [2023] suggesting that GDMs tend to learn data samples from high probability density regions in the data space and ignore the low probability density regions. However, many existing watermarks such FRQ Navas et al. [2008] and HiDDeN Zhu et al. [2018] can only generate distinct watermarks for different data samples without any relation between each other. In other words, their generated watermarks are dispersed and located in low-density areas in the data space. As a result, they cannot be effectively extracted and learned by GDMs. Therefore, in our work, we formally define the “*pattern uniformity*” as the consistency of different watermarks injected for different samples:

$$Z = 1 - \frac{1}{n} \sum_{i=1}^n \left\| \frac{\mathbf{W}_i}{\|\mathbf{W}_i\|_2} - \mathbf{W}_{mean} \right\|_2, \text{ where } \mathbf{W}_{mean} = \frac{1}{n} \sum_{i=1}^n \frac{\mathbf{W}_i}{\|\mathbf{W}_i\|_2} \quad (1)$$

where Z inversely corresponds to the standard deviation of normalized watermarks. A larger Z represents less diverse and higher pattern uniformity.

We further conduct experiments to illustrate the importance of this “*pattern uniformity*”. In the experiment shown in Figure 3, we test the ability of DDPM Ho et al. [2020] to learn watermarks with

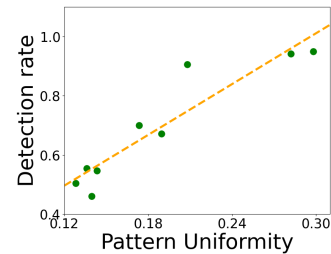


Figure 3: Pattern uniformity vs. watermark detection rate.

different pattern uniformity. The watermarks \mathbf{W}_i are random pictures whose pixel value is re-scaled by the budget σ to a limited range, and the watermarked images are $\tilde{\mathbf{X}}_i = \mathbf{X}_i + \sigma \times \mathbf{W}_i$. More details about the settings for this watermarks and the detector can be found in Appendix B.1. Figure 3 illustrates a positive correlation between the watermark detection rate in the GDM-generated images and the pattern uniformity, which implies that higher pattern uniformity facilitates better watermark reproduction. Motivated by this finding, we propose a novel watermarking approach characterized by high pattern uniformity, specifically designed to enhance protection against GDMs.

3.3 Watermarks and Decoding Watermarks

In this subsection, we introduce our proposed approach, referred as DiffusionShield. This model is designed to resolve the problem of inadequate reproduction of prior watermarking approaches in GDM-generated images. It adopts a blockwise watermarking approach to augment pattern uniformity, which improves the reproduction of watermarks in generated images and enhances flexibility.

Blockwise watermarks. In DiffusionShield, we use the sequence of *basis patches* to encode the textual copyright message M . In detail, the message M can be converted into a sequence of binary numbers by predefined rules like ASCII. To condense the sequence’s length, we convert the binary sequence into a B -nary sequence, denoted as $\{\mathbf{b}_{1:m}\}$, where m is the message length and B -nary represents different numeral systems like quaternary ($B = 4$) and octal ($B = 8$). Accordingly, DiffusionShield partitions the whole watermark \mathbf{W} into a sequence of m patches, $\{\mathbf{w}_{1:m}\}$, and each patch is chosen from a set of basis patch $\{\mathbf{w}^{(1:B)}\}$. The set $\{\mathbf{w}^{(1:B)}\}$ has B basis patch candidates with a shape (u, v) , which represent different values of the B -nary bits. The sequence of $\{\mathbf{w}_{1:m}\}$ denotes that of B -nary bits $\{\mathbf{b}_{1:m}\}$ derived from M . For example, as depicted in Figure 4, we have four basis patches ($B = 4$), and each of the patches has a unique pattern. To encode the copyright message $M = \text{“37th NeurIPS2023”}$, we first convert it into binary sequence $\text{“00110011 00110111 01110100...”}$ based on ASCII, and transfer it into quaternary sequence $\{\mathbf{b}_{1:m}\}$, “030303131310...” . Then we concatenate these basis patches in the order of $\{\mathbf{b}_{1:m}\}$ to get the complete watermark \mathbf{W} and add \mathbf{W} to the images from the data owner. Once the data offender uses a GDM to learn from it, the watermarks will appear on the generated images, serving as evidence of copyright infringement.

Decoding the watermarks. To detect the watermark and decode the message from the watermark, DiffusionShield employs a decoder, \mathcal{D}_θ , which is a classifier that can decode \mathbf{w}_i into a bit \mathbf{b}_i . Here, θ is the parameter of the classifier. \mathcal{D}_θ accepts an image block, \mathbf{x} , which is watermarked by a basis patch as input and outputs the category of the basis patch, i.e., $\mathbf{b}_i = \mathcal{D}_\theta(\mathbf{x}_i + \mathbf{w}_i)$. The sequence $\{\hat{\mathbf{w}}_{1:m}\}$ in the generated sample is classified into $\{\hat{\mathbf{b}}_{1:m}\} = \{\mathcal{D}_\theta(\hat{\mathbf{x}}_i + \hat{\mathbf{w}}_i) | i = 1, \dots, m\}$, which is the B -nary message that we embed into the watermark. With the decoded message, we can accurately identify the owner of the data, thereby confirming its origin. Our watermark can be reproduced in the generated samples when the protected data is trained by a GDM. In the generated samples, if the copyright information can be decoded by \mathcal{D}_θ , we can verify the infringement of GDM.

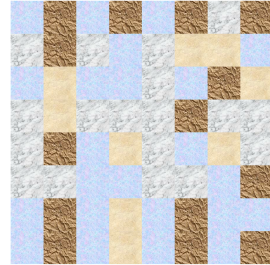


Figure 4: An 8×8 sequence of basis patches encoded with message “030303131310...” . Different patterns represent different basis patches.

Remarks. From the discussion above, it is evident that the designed watermarks have higher uniformity. It is because each user has the same watermark in their images. Therefore, these basis blocks and watermarks are more likely to be learned by GDMs. Additionally, DiffusionShield demonstrates remarkable flexibility when applied to multiple-owner scenarios since the basis patches and decoder can be reused by new owners. Once the watermarks are generated and the decoder is obtained, new users can form the new sequence of these basis patches without re-training.

3.4 Jointly Optimize Watermark and Decoder

While pattern uniformity facilitates the reproduction of watermarks in GDM-generated images, it does not guarantee the detection performance of the decoder, \mathcal{D}_θ . Therefore, we further propose a joint optimization method to search for the optimal basis patch patterns and obtain the optimized detection decoder in this subsection. Ideally, the basis patches and the decoder should satisfy:

$$\mathbf{b}^{(i)} = \mathcal{D}_\theta(\mathbf{p} + \mathbf{w}^{(i)}) \text{ for } \forall i \in \{1, 2, \dots, B\}, \quad (2)$$

where $\mathbf{w}^{(i)}$ is one of the B basis patch candidates, $\mathbf{b}^{(i)}$ is the correct label for $\mathbf{w}^{(i)}$, and \mathbf{p} can be a random block with the same shape as $\mathbf{w}^{(i)}$ cropped from any image. The ideal decoder, capable of accurately predicting all the watermarked blocks, ensures that all embedded information can be decoded from the watermark. To increase the detection performance of the decoder, we simultaneously optimize the basis patches and the decoder using the following bi-level objective:

$$\min_{\mathbf{w}^{1:B}} \min_{\theta} \mathbb{E} \left[\sum_{i=1}^B -\mathbb{1} \left[\mathcal{D}_{\theta} \left(\mathbf{p} + \mathbf{w}^{(i)} \right) = \mathbf{b}^{(i)} \right] \log \left(\mathcal{D}_{\theta, (i)} \left(\mathbf{p} + \mathbf{w}^{(i)} \right) \right) \right] \text{ s.t. } \|\mathbf{w}^{(i)}\|_{\infty} \leq \epsilon, \quad (3)$$

where the inner formulation is the cross-entropy loss for the classification of the basis patches, $\mathbb{1}$ is the indicator function, and $\mathcal{D}_{\theta, i}$ is the softmax probability for the i -th class. The l_{∞} budget is constrained by ϵ . To reduce the number of categories of basis patches, we set $\mathbf{w}^{(1)} = \mathbf{0}$, which means that the blocks without watermark should be classified as $\mathbf{b} = 1$. Thus, the bi-level optimization problem can be rewritten as:

$$\left\{ \begin{array}{l} \theta^* = \arg \min_{\theta} \mathbb{E} \left[\sum_{i=1}^B -\mathbb{1} \left[\mathcal{D}_{\theta} \left(\mathbf{p} + \mathbf{w}^{(i)} \right) = \mathbf{b}^{(i)} \right] \log \left(\mathcal{D}_{\theta, (i)} \left(\mathbf{p} + \mathbf{w}^{(i)} \right) \right) \right] \\ \mathbf{w}^{(2:B),*} = \arg \min_{\mathbf{w}^{(2:B)}} \mathbb{E} \left[\sum_{i=2}^B -\mathbb{1} \left[\mathcal{D}_{\theta^*} \left(\mathbf{p} + \mathbf{w}^{(i)} \right) = \mathbf{b}^{(i)} \right] \log \left(\mathcal{D}_{\theta^*, (i)} \left(\mathbf{p} + \mathbf{w}^{(i)} \right) \right) \right] \text{ s.t. } \|\mathbf{w}^{(i)}\|_{\infty} \leq \epsilon \end{array} \right. \quad (4)$$

The upper-level objective aims to increase the performance of the classifier \mathcal{D}_{θ} , while the lower-level objective optimizes the basis patches to facilitate their detection by the decoder. By the two levels of the objectives, the basis patches and the decoder potentially promote each other to achieve higher accuracy on a smaller budget. To ensure the basis patches can be adapted to various image blocks and thereby increase their flexibility, we use randomly cropped image blocks as the host images in the training process of the basis patches and decoder. More details about the algorithm of the joint optimization can be found in Appendix C.

4 Experiment

In this section, we assess the efficacy of DiffusionShield across various budgets, datasets, and protection scenarios. We first introduce our experimental setups in Section 4.1. In Section 4.2, we evaluate and analyze the performance of DiffusionShield in terms of its performance and invisibility during both the protection and audit stages. Then we further investigate DiffusionShield from Section 4.3 to Section 4.5 in terms of its flexibility and efficacy in multiple-user cases, its capacity for message length and robustness against image corruptions and GDM sampling accelerators, respectively.

4.1 Experimental Settings

Datasets, baselines and GDM. We conduct the experiments using three datasets and compare DiffusionShield with four baseline methods. The datasets include CIFAR10 and CIFAR100, both with $(U, V) = (32, 32)$ and STL10 with $(U, V) = (64, 64)$. The baseline methods include a simplified version of DiffusionShield without joint optimization called Image Blending (IB), DWT-DCT-SVD based watermarking in the frequency domain (FRQ) Navas et al. [2008], HiDDeN Zhu et al. [2018], and DeepFake Fingerprint Detection (DFD) Yu et al. [2021] (which is designed for DeepFake Detection and adapted to our data protection goal). In the audit stage, we use the improved DDPM proposed by Nichol et al. Nichol and Dhariwal [2021] as the GDM model to train on the watermarked data. More details about the baselines and the improved DDPM is in Appendix B.3 and B.4, respectively.

Evaluation metrics. In our experiments, we generate T images from each GDM and decode copyright messages from them. We compare the effectiveness of watermarks in terms of their invisibility, the decoding performance, and the capacity to embed longer messages:

- **(Perturbation) Budget.** We use the LPIPS Zhang et al. [2018] metric together with l_2 and l_{∞} differences to measure the visual discrepancies between the original and watermarked images. The lower values of these metrics indicate better invisibility.
- **(Detection) Accuracy.** Following Yu et al. [2021], Zhao et al. [2023b], we apply bit accuracy to evaluate the correctness of copyright messages encoded in the generated images. To

Table 1: Bit accuracy (%) and budget of the watermark

		IB	FRQ	HiDDeN	DFD	DiffusionShield (ours)				
CIFAR10	Budget	l_∞	7/255	13/255	65/255	28/255	1/255	2/255	4/255	8/255
		l_2	0.52	0.70	2.65	1.21	0.18	0.36	0.72	1.43
		LPIPS	0.01582	0.01790	0.14924	0.07095	0.00005	0.00020	0.00120	0.01470
	Accuracy	Released	87.2767	99.7875	99.0734	95.7763	99.6955	99.9466	99.9909	99.9933
		Cond.	87.4840	57.7469	98.9250	93.5703	99.8992	99.9945	100.0000	99.9996
		Uncond.	81.4839	55.6907	97.1536	89.1977	93.8186	95.0618	96.8904	96.0877
Pattern Uniformity		0.963	0.056	0.260	0.236	0.974	0.971	0.964	0.954	
CIFAR100	Budget	l_∞	7/255	14/255	75/255	44/255	1/255	2/255	4/255	8/255
		l_2	0.52	0.69	3.80	1.58	0.18	0.36	0.72	1.43
		LPIPS	0.00840	0.00641	0.16677	0.03563	0.00009	0.00013	0.00134	0.00672
	Accuracy	Released	84.6156	99.5250	99.7000	96.1297	99.5547	99.9297	99.9797	99.9922
		Cond.	54.3406	54.4438	95.8640	90.5828	52.0078	64.3563	99.8000	99.9984
		Uncond.	52.2786	55.5380	77.7616	77.7961	52.8320	54.4271	91.3021	87.2869
Pattern Uniformity		0.822	0.107	0.161	0.180	0.854	0.855	0.836	0.816	
STL10	Budget	l_∞	8/255	14/255	119/255	36/255	1/255	2/255	4/255	8/255
		l_2	1.09	1.40	7.28	2.16	0.38	0.76	1.51	3.00
		LPIPS	0.06947	0.02341	0.32995	0.09174	0.00026	0.00137	0.00817	0.03428
	Accuracy	Released	92.5895	99.5750	97.2769	94.2813	99.4969	99.9449	99.9762	99.9926
		Cond.	96.0541	54.3945	96.5164	94.7236	95.4848	99.8164	99.8883	99.9828
		Uncond.	89.2259	56.3038	91.3919	91.8919	82.5841	93.4693	96.1360	95.0586
Pattern Uniformity		0.895	0.071	0.155	0.203	0.924	0.921	0.915	0.907	

compute bit accuracy, we first transform the ground truth B -nary message $\{\mathbf{b}_{1:m}\}$ and the decoded message $\{\hat{\mathbf{b}}_{1:m}\}$ back into binary messages $\{\mathbf{b}'_{1:m \log_2 B}\}$ and $\{\hat{\mathbf{b}}'_{1:m \log_2 B}\}$. Then the bit accuracy for one watermark is calculated as:

$$\text{Bit-Acc} \equiv \frac{1}{m \log_2 B} \sum_{k=1}^{m \log_2 B} \mathbb{1}(\mathbf{b}'_{1:m \log_2 B} = \hat{\mathbf{b}}'_{1:m \log_2 B}). \quad (5)$$

The worst bit accuracy is expected to be 50%, which is equivalent to random guessing.

- **Message length.** The length of encoded message reflects the capacity of encoding. Apart from FRQ and HiDDeN, we encode a 128-bit message into each image of CIFAR10 and CIFAR100, and a 512-bit message into each image of STL10. To ensure the bit accuracy of FRQ and HiDDeN, we use 32 bits for CIFAR images and 64 bits for STL10.

Implementation details. We set $(u, v) = (4, 4)$ as the shape of the basis patches and set $B = 4$ for quaternary messages. We use ResNet He et al. [2016] as the decoder to classify different basis patches. For the joint optimization, we use 5-step PGD Madry et al. [2017] limited by $l_\infty \leq \epsilon$ to update the basis patches and use SGD to optimize the decoder. For training the GDMs, we consider the scenario where the data offender may collect and train the watermarked images and non-watermarked images together, as mentioned in Section 3.1. Hence, in all the datasets, we designate one random class of images as watermarked images, while treating other classes as unprotected images. To generate images of the protected class, we either 1) directly use a **class-conditional** GDM to generate images from the specified class, or 2) apply an object classifier to filter images of the protected class from the **unconditional** GDM’s output. The bit accuracy on unconditionally generated images may be lower than that of the conditional generated images because object classifiers cannot achieve 100% accuracy. More details are presented in Appendix B.2.

4.2 Results on Protection Performance against GDM

In this subsection, we demonstrate that our DiffusionShield can provide much better protection than other methods in invisibility and bit accuracy by the experimental results in Table 1. We compare the results on two groups of images: (1) the originally released images with watermarks (**Released**) and (2) the generated images from GDMs trained on the watermarked data via class condition GDM or unconditional GDM (**Cond.** and **Uncond.**). Based on the results in Table 1, we can see:

First, DiffusionShield can protect the images with the highest bit accuracy and the lowest budget among all the methods. For example, on CIFAR10 and STL10, with all the budgets from 1/255 to 8/255, DiffusionShield can achieve almost 100% bit accuracy on released images and conditionally generated images, which is better than all the baseline methods. Even constrained by the smallest budget with an l_∞ norm of 1/255, DiffusionShield can still achieve a high successful reproduction



Figure 5: Watermarked images by DiffusionShield and baseline approaches. From those examples, we can see that HiDDeN and DFD cause very obvious distortion of the original images, while DiffusionShield is almost invisible especially when the budget is 1/255 or 2/255. More examples can be found at Appendix D.

rate. On CIFAR100, although DiffusionShield with 1/255 and 2/255 l_∞ budget cannot keep a high bit accuracy in generated images due to the small budget, DiffusionShield with an l_∞ budget of 4/255 achieves a higher bit accuracy in generated images with a much lower l_∞ difference and LPIPS than baseline methods. For baselines, FRQ cannot be reproduced by GDM, while HiDDeN and DFD require a much larger perturbation budget over DiffusionShield, which is also visualized in Figure 5. Despite having a larger budget and a naive blockwise watermark, the accuracy of IB is much worse than the DiffusionShield with 1/255 budget on CIFAR10 and STL10. The reason for this is that without joint optimization, the decoder cannot perform well on released images and thus cannot guarantee its accuracy on generated images. This indicates the importance of joint optimization in producing optimal basis patches and decoder to increase the accuracy while keeping a low budget.

Second, we also show that enforcing pattern uniformity can promote the reproduction of watermarks in generated images. In Table 1, we can see that the bit accuracy of the conditionally generated images watermarked by DiffusionShield is as high as that of released images except those with 1/255 and 2/255 budget on CIFAR100, which is due to the limited budget. In addition to DiffusionShield, IB’s accuracy in released data and conditionally generated data are also similar. This is because IB is a simplified version of our method without joint optimization and also has high pattern uniformity. In contrast, other methods without pattern uniformity all suffer from a drop of accuracy from released images to conditionally generated images, especially FRQ, which has pattern uniformity lower than 0.11 and an accuracy level on par with a random guess. This implies that the decoded information in watermarks with high pattern uniformity (e.g., IB and ours in CIFAR10 are higher than 0.95²) does not change much from released images to generated images and the watermarks can be exactly and easily captured by GDM. It is worthwhile to note that the performance drop on CIFAR100 in 1/255 and 2/255 budgets is also partially due to the low watermark rate. In fact, both a small budget and a low watermark rate can hurt the reproduction of watermarks in generated images, which is discussed in Appendix E.

4.3 Flexibility and Efficacy in Multiple-user Case

In this subsection, we demonstrate another advantage of DiffusionShield: being flexibly transferred to new users and maintaining good protection against GDMs. We assume that multiple copyright owners are using DiffusionShield to protect their images, and different copyright messages should be encoded into the images from different copyright owners. In Table 2, we use one class in the dataset as the first owner and the other classes as the new owners. The basis patches (with 4/255 l_∞ budget) and decoder are optimized on the first class and re-used to protect the new classes. Images within the same class have the same message embedded, while images from different classes have distinct messages embedded in them. This process of transferring from one class to the other classes does not take any additional calculation except reordering the basis patches according to different copyright messages, which is very efficient. We train class-conditional GDM on all of the protected data and get the average bit accuracy across classes. As shown in Table 2, on both CIFAR10 and CIFAR100, when we reorder the basis patches to protect the other 3 classes or 9 classes, the protection performance is almost the same as the one class case, with bit accuracy all close to 100%. In addition to its flexibility, this result also shows that

Table 2: Average bit accuracy (%) across different numbers of copyright owners (on class-conditional GDM).

owners	CIFAR-10	CIFAR-100
1	100.0000	99.8000
4	99.9986	99.9898
10	99.9993	99.9986

²The perfect pattern uniformity is 1.00 if all the watermarks are exactly the same. But the pixel values of the watermarked image may exceed the range of [0, 255], so we need to clip it to [0, 255], which hurts uniformity.

Table 3: Bit accuracy (%) under corruptions

	DFD	ours
No corruption	93.5703	99.9996
Gaussian noise	68.6332	81.9340
Low-pass filter	88.9383	99.8582
Greyscale	50.8180	99.8129
JPEG compression	62.5484	94.4461

Table 4: Bit accuracy (%) with speeding-up models

l_∞		CIFAR10	CIFAR100	STL10
1/255	Cond.	99.7824	52.4813	95.8041
	Uncond.	94.6761	52.2693	82.4564
2/255	Cond.	99.9914	64.5070	99.8299
	Uncond.	96.1927	53.4493	90.4317
4/255	Cond.	99.9996	99.8445	99.9102
	Uncond.	96.1314	92.3109	95.7027
8/255	Cond.	100.0000	99.9984	99.9885
	Uncond.	95.7021	92.2341	95.3009

our watermarks can protect each of the multiple users and can distinguish them clearly even when their data are mixed by the data offender. This is a crucial advantage since we cannot control how the offender might combine our released watermarked data with other datasets when training a GDM.

4.4 Capacity for Message Length

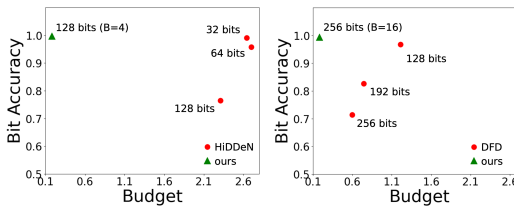
The capacity of embedding longer messages is important for watermarking methods since encoding more information can enhance protection by providing more conclusive evidence of infringement. In this subsection, we show the superiority of DiffusionShield over other methods in achieving high watermark capacity while maintaining a high bit accuracy and low budget. Here, we change the number of basis patches, B , to control the capacity of DiffusionShield and change the hyperparameters of HiDDeN and DFD to control their capacity. Figure 6 shows

the bit accuracy and l_2 budgets of watermarks with different message lengths on the released protected images in CIFAR10. In Figure 6a, we can see that HiDDeN consistently requires a large budget across varying message lengths, and its accuracy diminishes from 99% at 32 bits to 77% at 128 bits. Conversely, DiffusionShield maintains nearly 100% accuracy at 128 bits, even with a much smaller budget. Similarly, in Figure 6b, although DFD has a smaller budget than HiDDeN, its accuracy drops from 95% at 128 bits to 72% at 256 bits. In contrast, DiffusionShield maintains 99% accuracy at 256 bits, with significantly lower l_2 budget of 0.18. These observations indicate that DiffusionShield has significantly greater capacity compared to HiDDeN and DFD and can maintain good performance even with increased message lengths.

4.5 Robustness of DiffusionShield

Robustness of watermarks is important since there is a risk that the quality of the watermarks may be distorted by some disturbances, such as image corruption due to deliberate post-processing activities during the images’ circulation, or the application of speeding-up sampling methods in the GDM. In this subsection, we demonstrate that DiffusionShield is robust to maintain its bit accuracy on generated images when the images are corrupted or the sampling procedure is fastened.

Robustness against image corruptions. We consider Gaussian noise, low-pass filter, greyscale and JPEG compression to test the robustness of DiffusionShield against image corruptions. Different from the previous experiments, during the protection stage, we augment our method by incorporating corruptions into the joint optimization. Each corruption is employed after the basis patches are added to the images. Table 3 shows the bit accuracy of DiffusionShield (with an l_∞ budget of 8/255) on corrupted generated images. The results are compared with DFD, which also claimed robustness of their scheme. As shown by the results, DiffusionShield maintains around 99.8% accuracy under greyscale and low-pass filter, nearly matching the accuracy achieved without any corruption. In contrast, DFD performs nearly at the level of random guess under greyscale and only achieves an accuracy of 88.9383% under low-pass filter. Although DiffusionShield does experience some information loss under Gaussian noise and JPEG compression, with an accuracy of 81.9340% and 94.4461% respectively, its robust bit accuracy still surpasses DFD by about 13% under Gaussian noise and 32% under JPEG compression. From these results, we can see that DiffusionShield is robust against different image corruptions.



(a) HiDDeN & ours (1/255) (b) DFD & ours (1/255)
Figure 6: Bit acc. and l_2 of different message lengths

Robustness under speeding-up sampling models. Speeding-up sampling is often employed by practical GDMs due to the time-consuming nature of the complete sampling process, which requires thousands of steps. However, the quality of the images generated via speeded-up methods, such as Denoising Diffusion Implicit Model (DDIM) Song et al. [2020], is typically lower than normal sampling, which could destroy the watermarks on the generated images. In Table 4, we show the performance of DiffusionShield with DDIM to demonstrate its robustness against speeding-up sampling. Although DiffusionShield has low accuracy on CIFAR100 when the budget is 1/255 and 2/255 (same as the situation in Section 4.2), it can maintain high accuracy on all the other budgets and datasets. Even with a 1/255 l_∞ budget, the accuracy of DiffusionShield on CIFAR10 is still more than 99.7% in class-conditionally generated images and more than 94.6% in unconditionally generated images. This is because the easy-to-learn uniform patterns are learned by GDMs prior to other diverse semantic features like shape and textures. Thus, as long as DDIM can generate images with normal semantic features, our watermark can be reproduced in these images.

5 Conclusion and Limitations

In this paper, we introduce DiffusionShield, a blockwise watermark to protect data copyright against GDMs, which is motivated by our observation that the pattern uniformity can effectively assist the watermark to be captured by GDMs. By enhancing the pattern uniformity of watermarks and leveraging a joint optimization method, DiffusionShield successfully secures copyright with better accuracy and a smaller budget. Experimental results demonstrate the superior performance of DiffusionShield. More discussions on its social impact can be found at Appendix F. However, DiffusionShield currently has its limitations. It is primarily designed for GDMs trained from scratch, and its effectiveness may not extend to GDMs that are fine-tuned from pre-trained models, such as Stable Diffusion Rombach et al. [2022]. In addition, the performance of DiffusionShield is also influenced by the watermark rate. Our future work will focus on solving the limitations and enhancing its effectiveness and applicability.

References

- Jonathan Ho, Ajay Jain, and Pieter Abbeel. Denoising diffusion probabilistic models. *Advances in Neural Information Processing Systems*, 33:6840–6851, 2020.
- Aditya Ramesh, Prafulla Dhariwal, Alex Nichol, Casey Chu, and Mark Chen. Hierarchical text-conditional image generation with clip latents. *arXiv preprint arXiv:2204.06125*, 2022.
- Robin Rombach, Andreas Blattmann, Dominik Lorenz, Patrick Esser, and Björn Ommer. High-resolution image synthesis with latent diffusion models. In *Proceedings of the IEEE/CVF Conference on Computer Vision and Pattern Recognition*, pages 10684–10695, 2022.
- Lvmin Zhang and Maneesh Agrawala. Adding conditional control to text-to-image diffusion models. *arXiv preprint arXiv:2302.05543*, 2023.
- Ingemar Cox, Matthew Miller, Jeffrey Bloom, and Chris Honsinger. Digital watermarking. *Journal of Electronic Imaging*, 11(3):414–414, 2002.
- Christine I Podilchuk and Edward J Delp. Digital watermarking: algorithms and applications. *IEEE signal processing Magazine*, 18(4):33–46, 2001.
- Jiren Zhu, Russell Kaplan, Justin Johnson, and Li Fei-Fei. Hidden: Hiding data with deep networks. In *Proceedings of the European conference on computer vision (ECCV)*, pages 657–672, 2018.
- KA Navas, Mathews Cheriyan Ajay, M Lekshmi, Tampy S Archana, and M Sasikumar. Dwt-dct-svd based watermarking. In *2008 3rd International Conference on Communication Systems Software and Middleware and Workshops (COMSWARE’08)*, pages 271–274. IEEE, 2008.
- Ning Yu, Vladislav Skripniuk, Sahar Abdelnabi, and Mario Fritz. Artificial fingerprinting for generative models: Rooting deepfake attribution in training data. In *Proceedings of the IEEE/CVF International conference on computer vision*, pages 14448–14457, 2021.
- Prafulla Dhariwal and Alexander Nichol. Diffusion models beat gans on image synthesis. *Advances in Neural Information Processing Systems*, 34:8780–8794, 2021.

- Jonathan Ho and Tim Salimans. Classifier-free diffusion guidance. *arXiv preprint arXiv:2207.12598*, 2022.
- Jiaming Song, Chenlin Meng, and Stefano Ermon. Denoising diffusion implicit models. *arXiv preprint arXiv:2010.02502*, 2020.
- Jia Deng, Wei Dong, Richard Socher, Li-Jia Li, Kai Li, and Li Fei-Fei. Imagenet: A large-scale hierarchical image database. In *2009 IEEE conference on computer vision and pattern recognition*, pages 248–255. Ieee, 2009.
- Fisher Yu, Ari Seff, Yinda Zhang, Shuran Song, Thomas Funkhouser, and Jianxiong Xiao. Lsun: Construction of a large-scale image dataset using deep learning with humans in the loop. *arXiv preprint arXiv:1506.03365*, 2015.
- Yandong Guo, Lei Zhang, Yuxiao Hu, Xiaodong He, and Jianfeng Gao. Ms-celeb-1m: A dataset and benchmark for large-scale face recognition. In *European conference on computer vision*, pages 87–102. Springer, 2016.
- James Vincent. Ai art copyright lawsuit: Getty images and stable diffusion, February 2023. URL <https://www.theverge.com/2023/2/6/23587393/ai-art-copyright-lawsuit-getty-images-stable-diffusion>. Accessed: May 12, 2023.
- Frank Y Shih and Scott YT Wu. Combinational image watermarking in the spatial and frequency domains. *Pattern Recognition*, 36(4):969–975, 2003.
- Ashwani Kumar. A review on implementation of digital image watermarking techniques using lsb and dwt. *Information and Communication Technology for Sustainable Development: Proceedings of ICT4SD 2018*, pages 595–602, 2020.
- Ru Zhang, Shiqi Dong, and Jianyi Liu. Invisible steganography via generative adversarial networks. *Multimedia tools and applications*, 78:8559–8575, 2019.
- Matthew Tancik, Ben Mildenhall, and Ren Ng. Stegastamp: Invisible hyperlinks in physical photographs. In *Proceedings of the IEEE/CVF conference on computer vision and pattern recognition*, pages 2117–2126, 2020.
- Xinyu Weng, Yongzhi Li, Lu Chi, and Yadong Mu. High-capacity convolutional video steganography with temporal residual modeling. In *Proceedings of the 2019 on international conference on multimedia retrieval*, pages 87–95, 2019.
- Ian Goodfellow, Jean Pouget-Abadie, Mehdi Mirza, Bing Xu, David Warde-Farley, Sherjil Ozair, Aaron Courville, and Yoshua Bengio. Generative adversarial networks. *Communications of the ACM*, 63(11):139–144, 2020.
- Vikash Sehwal, Caner Hazirbas, Albert Gordo, Firat Ozgenel, and Cristian Canton. Generating high fidelity data from low-density regions using diffusion models. In *Proceedings of the IEEE/CVF Conference on Computer Vision and Pattern Recognition*, pages 11492–11501, 2022.
- Hanzhou Wu, Gen Liu, Yuwei Yao, and Xinpeng Zhang. Watermarking neural networks with watermarked images. *IEEE Transactions on Circuits and Systems for Video Technology*, 31(7): 2591–2601, 2020.
- Yuan Zhao, Bo Liu, Ming Ding, Baoping Liu, Tianqing Zhu, and Xin Yu. Proactive deepfake defence via identity watermarking. In *Proceedings of the IEEE/CVF Winter Conference on Applications of Computer Vision*, pages 4602–4611, 2023a.
- Jie Zhang, Dongdong Chen, Jing Liao, Han Fang, Weiming Zhang, Wenbo Zhou, Hao Cui, and Nenghai Yu. Model watermarking for image processing networks. In *Proceedings of the AAAI conference on artificial intelligence*, volume 34, pages 12805–12812, 2020.
- Yiming Li, Yang Bai, Yong Jiang, Yong Yang, Shu-Tao Xia, and Bo Li. Untargeted back-door watermark: Towards harmless and stealthy dataset copyright protection. *arXiv preprint arXiv:2210.00875*, 2022.

- Soobin Um and Jong Chul Ye. Don't play favorites: Minority guidance for diffusion models. *arXiv preprint arXiv:2301.12334*, 2023.
- Giannis Daras, Yuval Dagan, Alexandros G Dimakis, and Constantinos Daskalakis. Consistent diffusion models: Mitigating sampling drift by learning to be consistent. *arXiv preprint arXiv:2302.09057*, 2023.
- Alexander Quinn Nichol and Prafulla Dhariwal. Improved denoising diffusion probabilistic models. In *International Conference on Machine Learning*, pages 8162–8171. PMLR, 2021.
- Richard Zhang, Phillip Isola, Alexei A Efros, Eli Shechtman, and Oliver Wang. The unreasonable effectiveness of deep features as a perceptual metric. In *Proceedings of the IEEE conference on computer vision and pattern recognition*, pages 586–595, 2018.
- Yunqing Zhao, Tianyu Pang, Chao Du, Xiao Yang, Ngai-Man Cheung, and Min Lin. A recipe for watermarking diffusion models. *arXiv preprint arXiv:2303.10137*, 2023b.
- Kaiming He, Xiangyu Zhang, Shaoqing Ren, and Jian Sun. Deep residual learning for image recognition. In *Proceedings of the IEEE conference on computer vision and pattern recognition*, pages 770–778, 2016.
- Aleksander Madry, Aleksandar Makelov, Ludwig Schmidt, Dimitris Tsipras, and Adrian Vladu. Towards deep learning models resistant to adversarial attacks. *arXiv preprint arXiv:1706.06083*, 2017.

A Watermarking Protection for Multiple Copyright Owners

As shown in Algorithm 1, to extend the protection from the one-owner case to the multiple-owner case, we first build the watermark protection for one owner and get the corresponding watermark decoder \mathcal{D}_θ (line 1). Then we use the same procedure (that can be decoded by \mathcal{D}_θ) to watermark all the images from other owners (lines 2 to 4).

Algorithm 1 Watermark protection for multiple copyright owners

Input: The number of distinct sets of images to protect, K . Distinct sets, $\{\mathbf{X}_{1:n}^k\}$ and different copyright messages for different owners \mathbf{M}^k , where $k = 1, 2, 3, \dots, K$.

Output: Watermarked images $\{\tilde{\mathbf{X}}_{1:n}^k\}$, where $k = 1, 2, 3, \dots, K$ and the watermark decoder \mathcal{D}_θ .

- 1: $\{\tilde{\mathbf{X}}_{1:n}^1\}, \mathcal{D}_\theta \leftarrow \text{OneOwnerCaseProtection}(\{\mathbf{X}_{1:n}^1\}, \mathbf{M}^1)$
 - 2: **for** $k = 2$ to K **do**
 - 3: $\{\tilde{\mathbf{X}}_{1:n}^k\} \leftarrow \text{ReuseEncodingProcess}(\{\mathbf{X}_{1:n}^k\}, \mathbf{M}^k)$
 - 4: **end for**
 - 5: return $\{\tilde{\mathbf{X}}_{1:n}^k\}, k = 1, 2, 3, \dots, K$ and \mathcal{D}_θ .
-

B Additional Details of Experimental Settings

B.1 Watermarks and Detector of Experiment for Pattern Uniformity in Section 3.2

In the experiment shown in Figure 3, we test the ability of DDPM Ho et al. [2020] to learn watermarks with different pattern uniformity and show more details about the setting in this subsection.

Watermarks. We first choose one class from CIFAR10 as images requiring watermarks $\mathbf{X}_{1:R}$, where R is the number of images in this class and $R = 5000$ for CIFAR10. We randomly choose C images from 5 classes from CIFAR10 as $\mathbf{W}_{1:C}$, where C is the number of different watermarks and $C = 5, 10, 15, \dots$. Different watermarks are repeatedly added into $\mathbf{X}_{1:R}$ by $\tilde{\mathbf{X}}_i = \mathbf{X}_i + \sigma \times \mathbf{W}_i$. For example, we choose $C = 10$ images as watermarks and every watermark is used to watermark $R/C = 500$ images in $\mathbf{X}_{1:R}$. By choosing different C , we can control the uniformity. Larger C means more diverse watermarks and thus smaller pattern uniformity.

Detector. We train a classifier as the detector to detect the watermark in the generated images. The classifier is trained on the images watermarked by 10 classes. The label of the training images is set to be the watermark class. If the classifier predicts that the GDM-generated images have the watermark within the 5 classes from which the C watermarks are chosen, we see it as a successful detection, otherwise it is unsuccessful.

B.2 Decoder Architecture and Details about Training Parameters.

Given the small size of the blocks (4×4), we adapt the original ResNet structure by including only two residual blocks with 64 filters each, positioned between the initial convolutional layer and the global average pooling layer. In the joint optimization, for training decoder, we use the SGD optimizer with momentum to be 0.9, learning rate to be 0.01 and weight decay to be 5×10^{-4} , while for training watermark basis patches, we use 5-step PGD with step size to be 1/10 of the L_∞ budget.

B.3 Details of Baselines

Our method is compared with four existing watermarking methods although they are not specifically designed for the protection of image copyright against GDMs. Information on the baseline methods is provided as follows:

- **Image Blending (IB)**, a simplified version of our approach, which also applies blockwise watermark to achieve pattern uniformity but the patches are not optimized. Instead, it randomly selects some natural images, re-scales their pixel values to 8/255, and uses these as the basis patches. A trained classifier is also required to distinguish which patch is added to a block.

- **DWT-DCT-SVD based watermarking (FRQ)**, one of the traditional watermarking schemes based on the frequency domains of images. It uses Discrete Wavelet Transform (DWT) to decompose the image into different frequency bands, Discrete Cosine Transform (DCT) to separate the high-frequency and low-frequency components of the image, and Singular Value Decomposition (SVD) to embed the watermark by modifying the singular values of the DCT coefficients.
- **HiDDeN** Zhu et al. [2018], a neural network-based framework for data hiding in images. The model comprises a network architecture that includes an encoding network to hide information in an image, a decoding network to extract the hidden information from the image, and a noise network to attack the system, making the watermark robust.
- **DeepFake Fingerprint Detection (DFD)** Yu et al. [2021], a method for Deepfake detection and attribution (trace the model source that generated a deepfake). The fingerprint is developed as a unique pattern or signature that a generative model leaves on its outputs. It also employs an encoder and a decoder, both based on Convolutional Neural Networks (CNNs), to carry out the processes of watermark embedding and extraction.

B.4 Standard DDPM and Improved DDPM.

Standard DDPM. Denoising Diffusion Probabilistic Model (DDPM), firstly developed by Ho et al. [2020], consists of a diffusion process $q(x_t | x_{t-1})$ and a denoising process $p_\theta(x_{t-1} | x_t)$ which are respectively described as:

$$q(x_t | x_{t-1}) = \mathcal{N}\left(x_t; \sqrt{1 - \beta_t}x_{t-1}, \beta_t I\right) \quad (6)$$

$$p_\theta(x_{t-1} | x_t) = \mathcal{N}\left(x_{t-1}; \mu_\theta(x_t, t), \Sigma_\theta(x_t, t)\right) \quad (7)$$

With the variance schedule β_t , a data point x_0 sampled from a real data distribution is transformed into noise x_T by continuously adding a small amount of Gaussian noise to the sample for T steps. Then the image is gradually reconstructed by removing the noise from x_T following the reverse diffusion process 7.

The most effective way to parameterize $\mu_\theta(x_t, t)$ is to predict the noise added to x_0 in each step with a neural network. In practice, we use the simplified objective suggested by Ho et al. [2020]

$$L_t^{\text{simple}} = \mathbb{E}_{t \sim [1, T], \mathbf{x}_0, \epsilon_t} \left[\|\epsilon_t - \epsilon_\theta(\sqrt{\alpha_t}\mathbf{x}_0 + \sqrt{1 - \alpha_t}\epsilon_t, t)\|^2 \right] \quad (8)$$

Then the denoising process can be described as:

$$\mathbf{x}_{t-1} = \frac{1}{\sqrt{\alpha_t}} \left(\mathbf{x}_t - \frac{1 - \alpha_t}{\sqrt{1 - \alpha_t}} \epsilon_\theta(\mathbf{x}_t, t) \right) + \sigma_t \mathbf{z} \quad (9)$$

Improved DDPM. Nichol and Dhariwal [2021] proposed a few modifications of DDPM to achieve faster sampling speed and better log-likelihoods. The primary modification is to turn $\Sigma_\theta(x_t, t)$ into a learned function using the formula

$$\Sigma_\theta(x_t, t) = \exp\left(v \log \beta_t + (1 - v) \log \tilde{\beta}_t\right). \quad (10)$$

Moreover, they proposed a hybrid training objective

$$L_{\text{hybrid}} = L_t^{\text{simple}} + \lambda L_{\text{vlb}} \quad (11)$$

where L_{vlb} refers to the variational lower-bound of DDPM. To reduce the variance of the training log loss of L_{vlb} , they proposed importance sampling:

$$L_{\text{vlb}} = E_{t \sim p_t} \left[\frac{L_t}{p_t} \right], \text{ where } p_t \propto \sqrt{E[L_t^2]} \text{ and } \sum p_t = 1 \quad (12)$$

Finally, they introduced an enhancement to the noise schedule with:

$$\bar{\alpha}_t = \frac{f(t)}{f(0)}, \quad f(t) = \cos\left(\frac{t/T + s}{1 + s} \cdot \frac{\pi}{2}\right)^2 \quad (13)$$

C Algorithm

As shown in Algorithm 2, the joint optimization is numerically solved by alternately training on the two levels. Every batch is first watermarked and trained on the classifier for upper level objective by gradient descent (line 4 to 6), and then optimized on basis patches for lower level objective by 5-step PGD (line 7 to 9). With the joint optimized basis patches and classifier, we can obtain a robust watermark that can encode different ownership information with a small change on the protected data. This watermark can be easily captured by the diffusion model and is effective for tracking data usage and copyright protection. The clean images $\{\mathbf{X}_{1:n}\}$ for input of the algorithm is not necessary to be the images that we want to protect. The random cropped image blocks can help the basis patches to fit different image blocks and then increase the flexibility.

Algorithm 2 Joint optimization on $\{\mathbf{w}^{(1:B)}\}$ and \mathcal{D}_θ

Input: Initialized basis patches $\{\mathbf{w}_{(0)}^{(1:B)}\}$, clean images $\{\mathbf{X}_{1:n}\}$, upper and lower level objectives in Eq. 4, $\mathcal{L}_{\text{upper}}$, $\mathcal{L}_{\text{lower}}$, watermark budget ϵ , decoder learning rate r , batch size bs , PGD step α and epoch E .

Output: Optimal $\{\mathbf{w}^{(1:B),*}\}$ and θ^* .

- 1: $step \leftarrow 0$
- 2: **for** $epoch=1$ to E **do**
- 3: **for** $Batch$ from $\{\mathbf{X}_{1:n}\}$ **do**
- 4: $\{\mathbf{p}_{1:bs}\} \leftarrow \text{RandomCropBlock}(Batch)$
- 5: $\{\mathbf{w}_{1:bs}, \{\mathbf{b}_{1:bs}\} \leftarrow \text{RandomPermutation}(\{\mathbf{w}_{(step)}^{(1:B)}\}, bs)$
- 6: $\theta \leftarrow \text{StochasticGradientDescent}(\frac{\partial \sum_1^{bs} \mathcal{L}_{\text{lower}}(\mathbf{p}_i + \mathbf{w}_i, \mathbf{b}_i, \theta)}{\partial \theta}, r)$ // Training on classifier
- 7: **for** 1 to 5 **do**
- 8: $\mathbf{w}_{(step)}^{(2:B)} \leftarrow \mathbf{w}_{(step)}^{(2:B)} - \alpha \text{sign}(\frac{\partial \sum_1^{bs} \mathcal{L}_{\text{lower}}(\mathbf{p}_i + \mathbf{w}_i, \mathbf{b}_i, \theta)}{\partial \mathbf{w}_{(step)}^{(2:B)}})$ // 5-step Projected Gradient Descent
- 9: **end for**
- 10: $step \leftarrow step + 1$
- 11: **end for**
- 12: return $\{\mathbf{w}_{(step)}^{(1:B)}\}$ and θ .
- 13: **end for**

D Examples of Watermarked Images

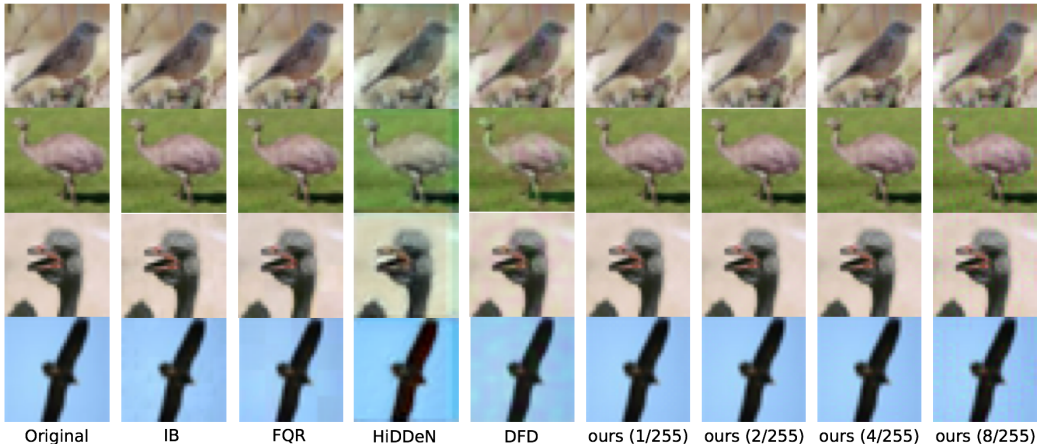


Figure 7: Examples of watermarked images of the bird class in CIFAR-10

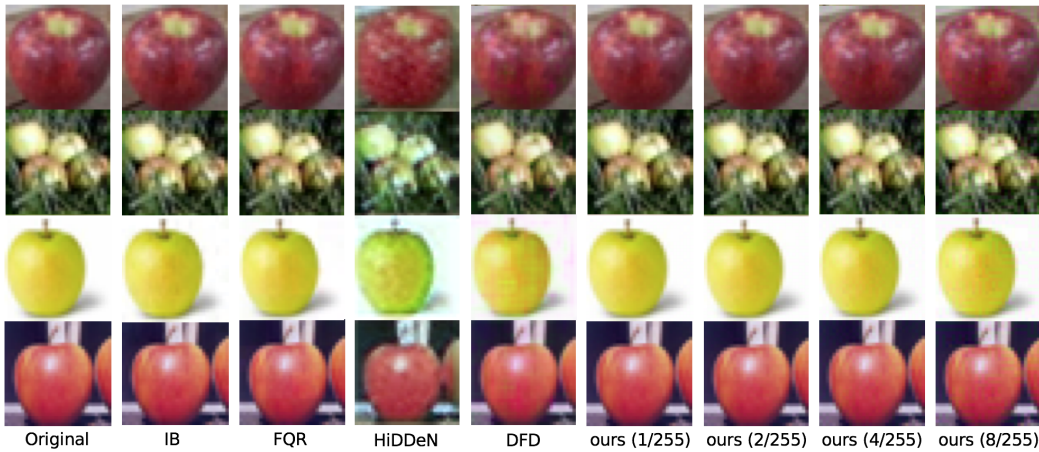


Figure 8: Examples of watermarked images of the apple class in CIFAR-100



Figure 9: Examples of watermarked images of the plane class in STL-10

E Additional Analysis on the Influence of Budget and Watermark Rate

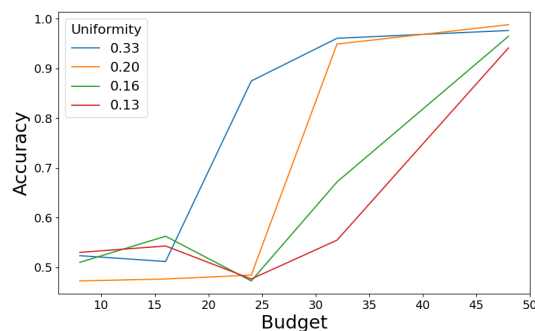


Figure 10: The change of bit accuracy under different budgets

As mentioned in Section 4.2, the reproduction of watermarks in generated images is related to the watermark budget and the watermark rate. In this subsection, we show that a larger budget and larger watermark rate can help with the reproduction of watermarks in the GDM-generated images.

In Figure 10, we follow the experimental setting in Section 3.2. We can see that when uniformity is the same, as the budget increases, the detection rate is also increasing, which means that watermarks can reproduce better if it has a larger budget. This can also be observed from Table 4.2 that the

bit accuracy of budget $1/255$ and $2/255$ on CIFAR100 is lower than $4/255$ and $8/255$. Meanwhile, higher pattern uniformity can increase faster than lower pattern uniformity, which is consistent with Section 3.2.

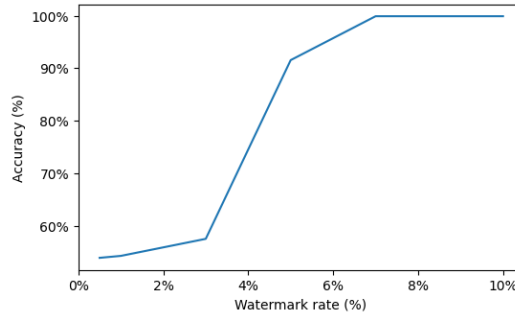


Figure 11: The change of bit accuracy with different watermark rates (budget=1/255)

In Figure 11, we follow the experimental setting in Section 4.1, while controlling the proportion of the watermarked images in the training set of GDM. From the figure, we can see that the bit accuracy on the generated images rises from about 53% to almost 100% when the watermark rate increases from 0.05% to 10%, which indicates that the watermark rate can affect the degree of reproduction of the watermark in generated images.

Figure 11 suggests that DiffusionShield cannot provide satisfied protection in the single-owner case when the watermark rate and the budget are small. In reality, the watermark rate for a single user may be small. However, there are multiple users who may adopt DiffusionShield to protect the copyright of their data. Therefore, next we check how the performance of DiffusionShield changes with the number of users when the watermark rate and the budget are small for each user. Although each user has a distinct set of watermarked data, they all share the same set of basis patches, which has the potential to enhance the reproducibility of the watermark. As shown in Figure 12, we have K owners and the images of each owner compose 1% of the collected training data. As the number of owners increases from 1 to 20, the average accuracy increases from about 64% to nearly 100%. This observation indicates that DiffusionShield can work with multiple users even when the watermark rate and the budget are small for each user. Since GDM often collects training data from multiple users, this study suggests that DiffusionShield could be very practical.

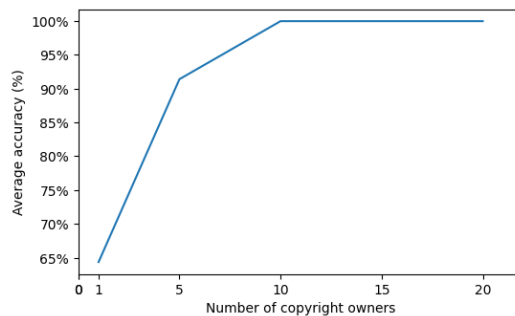


Figure 12: The change of bit accuracy with different numbers of copyright owners (budget=2/255)

F Boarder Impact of DiffusionShield

The development of DiffusionShield may have far-reaching implications across various domains.

1. **Art and creative industries.** The proposed watermarking scheme, DiffusionShield, holds immense potential for safeguarding the intellectual property of artists against unauthorized replication of their creative works by GDMs. It offers a much-needed solution to an emerging

problem in the digital age, where the line between creativity and plagiarism can be blurred by advanced technology.

2. **Generative model and AI community.** This paper paves the way for responsible and ethical use of GDMs. It can encourage researchers, developers, and users of GDMs to respect the intellectual property rights of creators, fostering a more ethical landscape within the AI community.
3. **Legal frameworks and policies.** The implementation of DiffusionShield could impact copyright laws and policies. It provides a technical solution to expose copyright infringement with concrete evidence, contributing to more effective enforcement of digital copyright laws.
4. **Digital media and information.** By ensuring that the ownership information is encoded within an imperceptible watermark, this technology can help maintain the integrity of media and information. It reduces the risk of misattributed or misrepresented content, which is especially crucial in today's digital age.